International Journal of Control and Automation
Vol. 9, No. 8 (2016), pp.261-270
http//dx.doi.org/10.14257/ijca.2016.9.8.25

Optimal Design of Low Gain Full State Feedback Control for DC-DC Converter

Liang Kangyou[1], Yuan Ling[2] and Tan Yuhang[3]

[1]*Chongqing University of Arts and Sciences, Chongqing Yongchuan, 402160, China*
[2]*Chongqing electric power company, Chongqing Yongchuan, 402160, China*
[3]*Chongqing University of Arts and Sciences, Chongqing Yongchuan, 402160, China*

Abstract

Buck converter is taken as an example to research the full state space design feedback vector optimization problem. The full state space design is extraordinarily effective for the pole configuration in the closed-loop system, but when such control thought is applied to DC-DC switching converter, the actuator cannot completely execute relevant action due to the limited control action thereof or even the closed-loop system becomes unstable due to actuator saturation. 2-norm based low gain pole configuration is proposed in this article to design the full state control system without static error, and meanwhile the low gain feedback vector is designed according to the state space equation in order to ensure that the system has good starting performance, good power supply adjustment rate and good load adjustment rate. The research result shows that the low gain pole configuration can not only satisfy the system requirement, but also has better control effect than the traditional PI control, namely with better dynamic adjustment characteristic and static error adjustment characteristic; meanwhile, the overshoot, the adjustment time, etc. are obviously improved to provide reference for controller design & optimization and facilitate engineering implementation.

Keywords*: Full State Feedback; Pole Configuration; 2-norm; Feedback Vector*

1. Introduction

As the basic component for constituting other electrical energy transformers, DC-DC converter is widely applied in such fields as photovoltaic power generation, aviation, aerospace, communication and computer. At present, the existing mature theories for DC-DC converter research are mainly focused on adopting the linear system theory for the small signal modeling for the switching converter and adopting the classic PID control theory for analyzing and designing the control system, thus to better solve the problems regarding the steady-state and dynamic low-frequency small signal analysis of DC/DC converter. However, the common PID control strategy is sensitive to the system parameter change, and especially during the starting process or under the condition of sudden load change, large load change, large power supply fluctuation or nonlinear load in the system, the switching converter has slow dynamic response speed, or the output waveform is seriously distorted, or even the system is instable, *etc*. [1-3]

The state variables are adopted in the modern control theory to disclose the internal characteristics of the system so as to establish a kind of new control structure and method based on the state feedback. Compared with the traditional control structures only depending on the output feedback to control and display the control system, such control structure has more advantages, because it integrates all

ISSN: 2005-4297 IJCA

state variable information of the system. Especially, the modern control strategy represented by the pole configuration has extraordinary control effect, thus becoming the development tendency of the high-quality control systems.

Although the pole configuration in the closed loop system in the modern control theory has extraordinary capability, but when such control thought is applied to DC-DC switching converter, the controller has high gain and the actuator cannot completely execute relevant action due to the limited control action thereof, or even the closed-loop system becomes instable due to actuator saturation. Therefore, it is necessary to research how to configure the poles in actual system in order to equally consider the above two problems. In this article, the low gain pole configuration is proposed, and meanwhile 2-norm is adopted to evaluate the configuration effect, thus to minimize the gain under the condition of meeting the transient-state and steady-state performance indexes and avoid or reduce the unexpected system response caused by the saturation characteristics of the actuator[2-4].

2. Pole Configuration Design for Dc-Dc Switching Converter

DC/DC switching converter can be described by the state space of Formula (1):

$$\begin{cases} \dot{\boldsymbol{x}} = \boldsymbol{A}\boldsymbol{x} + bu \\ y = \boldsymbol{c}\boldsymbol{x} \end{cases} \tag{1}$$

The controlled object is simply recorded as $\sum 0(\boldsymbol{A},\boldsymbol{b},\boldsymbol{c})$. Information xi(i=1,2,…,n) of n state variables is educed through the state feedback and fed back to the system reference input v through (1×n) feedback row vector K=[k0 k1…kn-1]. The state feedback structure control system of DC-DC switching converter is as shown in Figure 1.

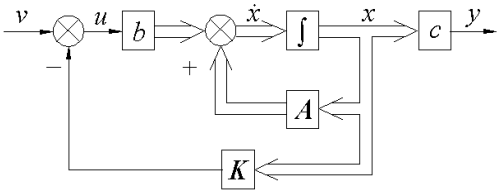

Figure 1. State Feedback Structure Diagram of DC-DC System

The necessary and sufficient conditions for adopting the state feedback to configure the closed-loop pole at any position are that the controlled object $\sum 0(\boldsymbol{A},\boldsymbol{b},\boldsymbol{c})$ can be completely controlled.

The linear state feedback control rate u is as follows:

$$u=v-\boldsymbol{K}\boldsymbol{x} \tag{2}$$

The above formula is put into Formula (1) to obtain the closed-loop system state space description of the state feedback:

$$\begin{cases} \dot{\boldsymbol{x}} = (\boldsymbol{A} - \boldsymbol{b}\boldsymbol{k})\boldsymbol{x} + \boldsymbol{b}v \\ y = \boldsymbol{c}\boldsymbol{x} \end{cases} \tag{3}$$

According to the above formula, after the state feedback is adopted, the original state equation is changed but the output equation is not changed. The closed-loop system is simply recorded as $\sum$k=[($\boldsymbol{A}$-$\boldsymbol{b}\boldsymbol{K}$),$\boldsymbol{b}$,$\boldsymbol{c}$]. This formula shows that the coefficient of the characteristic polynomial of the closed-loop system can be changed through the selection of the element value of the feedback vector K in order to change the characteristic value of the system, namely the closed-loop pole[4].

According to Formula (3) and Structure Diagram 1, if the system can be controlled and observed, then the state feedback gain matrix can be suitably selected to realize the pole configuration of the system, wherein the expected closed-loop

poles can be designed according to system stability and dynamic quality. According to the pole configuration result, the transient quality and the dynamic quality of the system are changed along with the pole change, but the steady-state quality of the system is not changed, namely: the output result of the system cannot satisfy the preset requirement of the system and the system has steady-state error. In order to solve the steady-state error problem of the system, the control objective of DC-DC switching converter shall be the output voltage thereof. According to the Structure Diagram 1, the output voltage of the controlled variable is not introduced into the system state feedback to be taken as the feedback variable. In order to enable the system to not only satisfy the preset requirement of the system, but also have the performance of conquering power supply disturbance and load disturbance, the output voltage feedback is introduced on the basis of the state feedback and meanwhile an integration element is added to the system, thus to change the system into I-type system. In this way, the system can not only achieve the steady-state error free performance index, but also achieve the transient-state performance index. In allusion to DC-DC switching converter, the structure diagram in Figure 1 can be changed as the structure diagram in Figure 2 to realize the system without steady-state error.

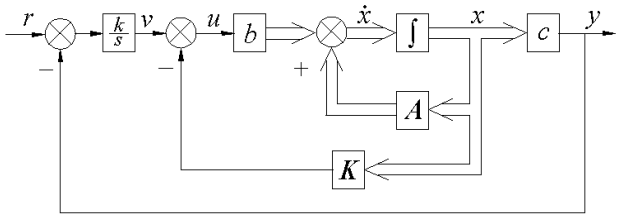

Figure 2. State Feedback Structure Diagram of DC-DC Switching Converter without Static Error

3. Low Gain Pole Configuration Design

The characteristics of the system transition process caused by the initial condition and the reference input directly depend on the poles, so the purpose of the pole configuration design is to enable the system transition process to attenuate and disappear within an acceptable period. If the system is controllable and all variables thereof can be used for feedback, then the full state feedback can be adopted to configure the poles of the closed-loops system at any position in *S* plane.

Although the controllable control system has extraordinary capability for the pole configuration of the closed-loop system, the limitation of the control action of the actuator shall be considered during the practical configuration process. Especially, in DC-DC switching converter, PWM control signal loaded on the fully-controlled switching element is obtained through the comparison between the feedback gain and the sawtooth wave, so if the controller has large gain, then the actuator cannot completely execute relevant action and the system will become instable due to actuator saturation. Since the pole configuration can generate excessive gain and make the actuator saturated, thus it is necessary to not only consider whether the configured system has excellent transient-state performance, but also consider the feasibility thereof. In conclusion, the transient-state performance and the steady-state performance shall be considered for the pole configuration of the system, and the implementation feasibility shall be also considered.

Therefore, during the pole configuration, we configure the closed-loop pole at the expected position near the open loop pole so that the system has relatively low gain and the state space control system can be probably realized. In order to measure the

amplitude of the gain vector ***K***, we adopt 2-norm for relevant measurement and define it as follows:

$$\|F\|_2 = (\sum_{i=1}^{n} K_i^2)^{1/2} \tag{4}$$

In the above formula, K_i is an element of ***F***.

4. Low Gain Pole Configuration for Buck Switching Converter

4.1. Pole Configuration Design for Buck Switching Converter Without Static Error

The main circuit topology of Buck DC-DC switching converter is as shown in Figure 3. As a Buck converter, this converter can convert the input voltage *U*i into [0~*U*i]. Buck converter circuit is a second-order circuit and has two state variables, namely inductive current and capacitor voltage. Specifically, the two state variables are selected for realizing the full state feedback, wherein the state variable *x*1 is as the inductive current *i*L, and the state variable *x*2 is set as the capacitor terminal voltage *u*o. According to the working characteristics of the circuit, the on-state and the off-state of the fully controlled component V are respectively corresponding to two state equations. Meanwhile, the two equations are weighted and averaged according to the proportions thereof when V is respectively in the on-state and in the off-state in order to obtain the mean state equation as shown in Formula (3).

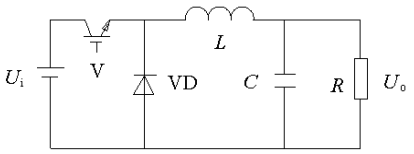

Figure 3. Buck DC-DC Switching Converter

$$\dot{x} = \begin{bmatrix} 0 & -\frac{1}{L} \\ \frac{1}{C} & -\frac{1}{RC} \end{bmatrix} \begin{bmatrix} x_1 \\ x_2 \end{bmatrix} + \begin{bmatrix} \frac{U_i}{L} \\ 0 \end{bmatrix} u$$

$$y = \begin{bmatrix} 0 & 1 \end{bmatrix} \begin{bmatrix} x_1 \\ x_2 \end{bmatrix} \tag{5}$$

Therein:

$$A = \begin{bmatrix} 0 & -\frac{1}{L} \\ \frac{1}{C} & -\frac{1}{RC} \end{bmatrix}, \quad b = \begin{bmatrix} \frac{U_i}{L} \\ 0 \end{bmatrix}, \quad C = \begin{bmatrix} 0 & 1 \end{bmatrix}$$

According to the structure diagram of DC-DC switching converter without static error as shown in Figure 2, we can obtain the structure diagram of Buck DC-DC switching converter without static error, as shown in Figure 4.

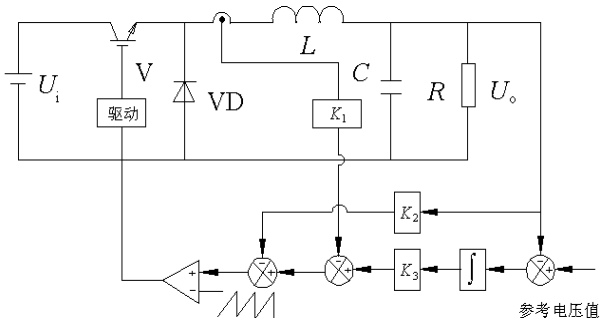

Figure 4. State Feedback System Diagram of Buck Switching Converter without Static Error

State space equation (5) of the original system is changed due to the change of the structure diagram. According to Figure 4, the state matrixes ***A*** and ***b*** of Buck switching converter at this moment are changed as follows:

$$\boldsymbol{A}' = \begin{bmatrix} 0 & -\frac{1}{L} & 0 \\ \frac{1}{C} & -\frac{1}{RC} & 0 \\ -1 & 0 & 0 \end{bmatrix}, \quad b' = \begin{bmatrix} \frac{U_i}{L} \\ 0 \\ 0 \end{bmatrix}$$

The matrix composed of $\boldsymbol{A'}$ **and** $\boldsymbol{b'}$ can be controlled and observed, so $\boldsymbol{A'}$ **and** $\boldsymbol{b'}$ can be adopted for the full state feedback pole configuration of the system.

4.2. Low Gain Pole Configuration K Design

The circuit parameters are given according to the full state feedback structure diagram of Buck switching converter without static error as shown in Figure 4, and the low gain feedback vector is designed according to the given parameters, wherein the circuit parameters are as follows: input voltage *U*i=20V, filter inductance *L*=1mH, filter capacitance *C*=10μF, load resistance *R*=10Ω, duty ratio D=0.5, switching frequency *f*s=150kHz, sawtooth wave Vm=2.4V, designed output voltage of the system *U*o=10V. According to the above given parameters, we can obtain the following calculation results for Buck converter: inherent closed-loop pole -5000±8660j; damping ratio δ=0.5, and *t*s=0.6ms.

According to Figure 4, three poles shall be configured at this moment, and the three poles to be configured are set as follows:

*S*1,2=a±bj; *S*3=na

Table 1 shows the values of 10 different groups of expected poles and feedback vectors of the system, namely feedback vector 2-norm. In order to make the given data have comparability, the expected poles *S*1,2 shall be configured to ensure that the expected closed-loop pole a is 0.4 multiples of pole b in each group (namely: ensure the same overshoot), and *S*3 shall be configured to ensure that the transition process caused by *S*3 real pole for each group of data has same attenuation rate. For the consideration of the rapidity of the system transition, it is necessary to select n=5.

According to Table 1, when the distance difference between the expected pole and the inherent pole of the system is 10 multiples (namely the first group of data and the ninth group of data), the feedback vector norm of the first group of data is 362,500 which is 100 multiples of the configuration result (362.5) of the ninth group of data near the inherent pole. According to the result comparison in the table, along

with the reduction of the distance between the expected pole configured thereby and the inherent pole of the original system, the 2-norm of the feedback vector *K* is sharply reduced. Therefore, during the pole configuration, we shall configure the pole near the inherent pole of the system as much as possible in order to significantly reduce the feedback vector. Meanwhile, the small feedback vector norm indicates the reduction of the actuator saturation caused by the feedback gain, namely: the system response is more consistent with the designed index requirements.

Table 1. Calculation of Feedback Vector of Expected Pole and 2-Norm

Expected Pole			Feedback Vector			Norm (F)
Pole 1	Pole 2	Pole 3	K1	K2	K3	
-50000+20000j	-50000-20000j	-250000	12.200	17.000	-262500	362500
-30000+12000j	-30000-12000j	-150000	3.9720	10.000	-78300	783000
-25000+10000j	-25000-10000j	-125000	2.6125	8.2500	-45312	45313
-20000+8000j	-20000-8000j	-100000	1.5320	6. 5000	-23200	23200
-16000+6400j	-16000-6400j	-80000	0.8685	5.1000	-11878	11878
-12000+4800j	-12000-4800j	-60000	0.3835	3.7000	-5011	5011
-10000+4000j	-10000-4000j	-50000	0.2080	3.0000	-2900	2900
-8000+3200j	-8000-3200j	-40000	0.0771	2.3000	-1485	1485
-5000+2000j	-5000-2000j	-25000	-0.0355	1.2500	-362.5	362.5
-5000+5000j	-5000-5000j	-25000	-0.0250	1.2500	-625	625

5. Simulation Verification of Low Gain Pole Configuration

Buck switching converter is taken as an example for the simulation verification, wherein the simulation circuit is as shown in Figure 4. Specifically, the simulation circuit parameters are as follows: *U*i=20V, *L*=1mH, *C*=10μF, *R*=10Ω, D=0.5, *f*s=150 kHz, Vm=2.4V. *U*o=10V; the simulation software PSIM6.0 dedicated for the power electronic circuit is selected as the simulation software.

In order to describe the effectiveness and the configuration effect of the low gain pole configuration, the transient-state effect and the steady-state effect of PI control are compared with those of the pole configuration in this article. Meanwhile, in order to verify the anti-interference performance of the low gain pole configuration system, the power supply adjustment rate and the load adjustment rate of PI control system are also compared with those of the pole configuration system in this article.

The controller parameters are as follows: PI controller parameters: *K*p=0.32, *K*i=10000; low gain pole controller parameters: the ninth group of expected poles in table ---- [-5000+2000j ; -5000-2000j ; -25000], feedback gain [*K*1, *K*2, *K*3]=[-0.0355 ; 1.25 ; 362.5].

Figure 5 shows the comparison of the transient-state characteristics and the power supply adjustment rate control effects of PI control system and the low gain pole configuration system during the starting process. According to Figure 5, the low gain pole configuration is superior to PI control during the system starting process in the aspects of rapidity and overshoot. In order to conveniently compare the power adjustment rates of the above two control systems, the voltage disturbance (±6V) is applied to the input power voltage at 5ms and at 10ms when the two control systems reach steady state. According to the simulation result comparison, the low gain pole configuration is obviously superior to PI control in the aspect of power supply adjustment rate.

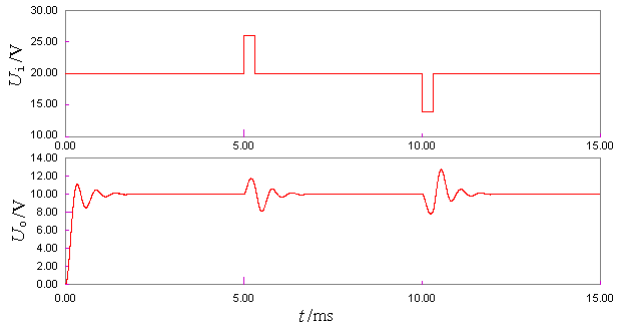

(a) Simulation of power supply adjustment rate of common PI control

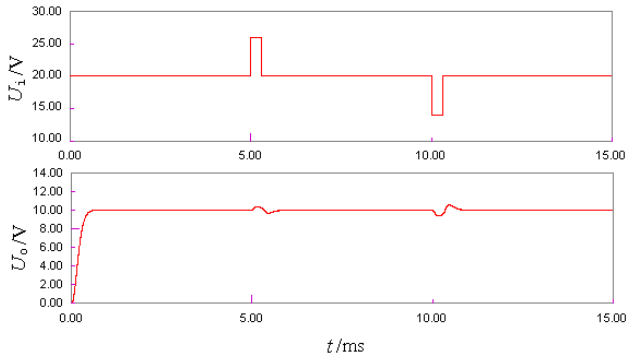

(b) Simulation of power supply adjustment rate of low gain pole configuration

Figure 5. Simulation Verification of System Starting and Power Supply Adjustment Rate

Figure 6 shows the comparison of the system load adjustment rate control effects of PI control and low gain pole configuration. In order to conveniently compare the load adjustment rate effects of the two control systems, when the two systems respectively reach the steady state, 15Ω load is connected in parallel to the original system load at 5ms (the original load is 10Ω, and the load is reduced as 6Ω at this moment), and 15Ω load is removed at 10ms (the load is changed as 10Ω at this moment).

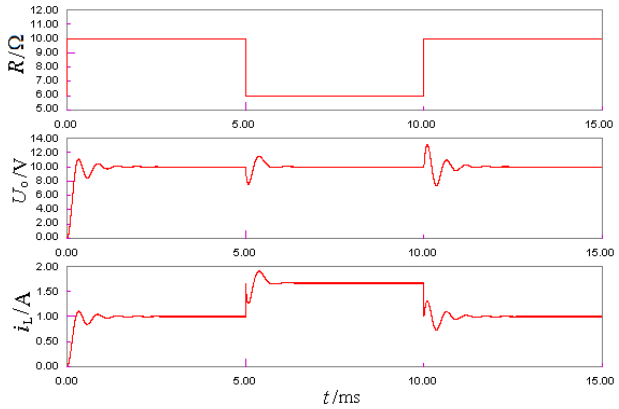

(a) Simulation of load adjustment rate of common PI control

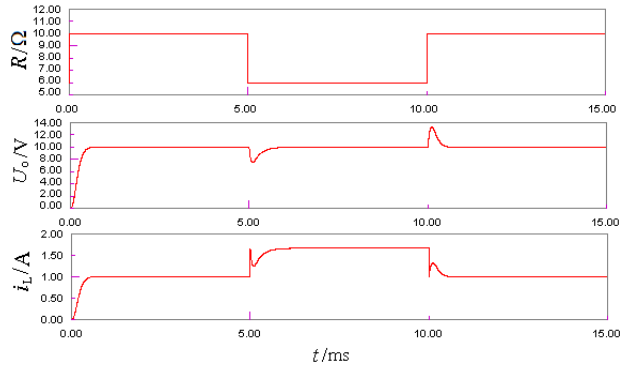

(b) Simulation of load adjustment rate of low gain pole configuration

Figure 6. Simulation Verification of System Load Adjustment Rate

According to Figure 6, when the low gain pole configuration and PI control have same load change, the low gain pole configuration has short dynamic transition process for the output voltage, small voltage drop and small load current change, thus to be superior to common PI control.

In conclusion, according to Figures 5 and 6, the low gain pole configuration is superior to traditional PI control in the aspects of system starting process, power supply disturbance resistance, load disturbance resistance. Meanwhile, the two figures also indicate that the low gain pole configuration is feasible.

6. Conclusion

The full state pole configuration based on state variables can realize the optional pole configuration for the system, and good transient-state effect and steady-state effects are obtained in the simulation experiment. However, the pole configuration can increase the feedback vector gain and accordingly saturates the controller, so the actual pole configuration effect is not ideal. In this article, 2-norm is introduced therein to optimize the pole configuration design in order to not only consider the transient-state characteristics and the steady-state characteristics of the system, but also maximally reduce the system feedback vector K, thus to provide relevant basis for realizing the full state feedback system and optimize DC-DC full state feedback vector design as well as provide the control parameter optimization basis for high-performance and high-quality DC-DC switching converter. The research result shows that the low gain pole configuration can not only have small feedback vector, but also enable the system to have good starting performance, good power supply adjustment rate and good load adjustment rate. Moreover, such research result has good application prospect in the high-performance control of such nonlinear system as power electronic system.

References

[1] J. Hu and Z.i Gao, "Distinction immune genes of hepatitis-induced heptatocellular carcinoma", Bioinformatics, vol. 28, no. 24, **(2012)**, pp. 3191-3194.
[2] J. Yang, B. Chen and J. Zhou, "A Low-Power and Portable Biomedical Device for Respiratory Monitoring with a Stable Power Source", Sensors, **(2015)**, vol. 15, no. 8, pp. 19618-19632.
[3] G. Bao, L. Mi, Y. Geng and K. Pahlavan, "A computer vision based speed estimation technique for localiz ing the wireless capsule endoscope inside small intestine", 36th Annual International Conference of the IEEE Engineering in Medicine and Biology Society (EMBC), **(2014)**.
[4] X. Song and Y. Geng, "Distributed community detection optimization algorithm for complex networks", Journal of Networks, vol. 9, no. 10, **(2014)**, pp. 2758-2765.
[5] D. Jiang, X. Ying and Y. Han, "Collaborative multi-hop routing in cognitive wireless networks", Wireless Personal Communications, **(2015)**, pp. 1-23.

[6] Z. Lv, A. Halawani and S. Feng, "Multimodal hand and foot gesture interaction for handheld devices", ACM Transactions on Multimedia Computing, Communications, and Applications (TOMM), vol. 11, no. 1s, **(2014)**, pp. 10.
[7] G. Liu, Y. Geng and K. Pahlavan, "Effects of calibration RFID tags on performance of inertial navigation in indoor environment", 2015 International Conference on Computing, Networking and Communications (ICNC), **(2015)**.
[8] J. He, Y. Geng, Y. Wan, S. Li and K. Pahlavan, "A cyber physical test-bed for virtualization of RF access environment for body sensor network", IEEE Sensor Journal, vol. 13, no. 10, **(2013)**, pp. 3826-3836.
[9] W. Huang and Y. Geng, "Identification Method of Attack Path Based on Immune Intrusion Detection", Journal of Networks, vol. 9, no. 4, **(2014)**, pp. 964-971.
[10] X. Li, Z. Lv and J. Hu, "XEarth: A 3D GIS Platform for managing massive city information", Computational Intelligence and Virtual Environments for Measurement Systems and Applications (CIVEMSA), 2015 IEEE International Conference on. IEEE, **(2015)**, pp. 1-6.
[11] J. He, Y. Geng, F. Liu and C. Xu, "CC-KF: Enhanced TOA Performance in Multipath and NLOS Indoor Extreme Environment", IEEE Sensor Journal, vol. 14, no. 11, **(2014)**, pp. 3766-3774.
[12] N. Lu, C. Lu, Z. Yang and Y. Geng, "Modeling Framework for Mining Lifecycle Management", Journal of Networks, vol. 9, no. 3, **(2014)**, pp. 719-725.
[13] Y. Geng and K. Pahlavan, "On the accuracy of rf and image processing based hybrid localization for wireless capsule endoscopy", IEEE Wireless Communications and Networking Conference (WCNC), **(2015)**.
[14] X. Li, Z. Lv and J.Hu, "Traffic management and forecasting system based on 3d gis", Cluster, Cloud and Grid Computing (CCGrid), 2015 15th IEEE/ACM International Symposium on, **(2015)**, pp. 991-998.
[15] S. Zhang and H. Jing, "Fast log-Gabor-based nonlocal means image denoising methods", Image Processing (ICIP), 2014 IEEE International Conference on. IEEE, **(2014)**, pp. 2724-2728.
[16] D. Jiang, Z. Xu and Z. Chen, "Joint time-frequency sparse estimation of large-scale network traffic", Computer Networks, **(2011)**, vol. 55, no. 15, pp. 3533-3547.J. Hu, Z. Gao and W. Pan, "Multiangle Social Network Recommendation Algorithms and Similarity Network Evaluation", Journal of Applied Mathematics, **(2013)**.
[17] J. Hu and Z. Gao. Modules identification in gene positive networks of hepatocellular carcinoma using Pearson agglomerative method and Pearson cohesion coupling modularity[J]. Journal of Applied Mathematics, 2012 **(2012)**.
[18] Z. Lv, A. Tek and F. Da Silva, "Game on, science-how video game technology may help biologists tackle visualization challenges", PloS one, vol. 8, no. 3, **(2013)**, pp. 57990.
[19] T. Su, W. Wang and Z. Lv, "Rapid Delaunay triangulation for randomly distributed point cloud data using adaptive Hilbert curve", Computers & Graphics, vol. 54, **(2016)**, pp. 65-74.
[20] S. Zhou, L. Mi, H. Chen and Y. Geng, "Building detection in Digital surface model", 2013 IEEE International Conference on Imaging Systems and Techniques (IST), **(2012)**.
[21] J. He, Y. Geng and K. Pahlavan, "Toward Accurate Human Tracking: Modeling Time-of-Arrival for Wireless Wearable Sensors in Multipath Environment", IEEE Sensor Journal, vol. 14, no. 11, **(2014)**, pp. 3996-4006.
[22] Z. Lv, A. Halawani and S. Fen, "Touch-less Interactive Augmented Reality Game on Vision Based Wearable Device", Personal and Ubiquitous Computing, vol. 19, no. 3, **(2015)**, pp. 551-567.
[23] G. Bao, L. Mi, Y. Geng, M. Zhou and K. Pahlavan, "A video-based speed estimation technique for localizing the wireless capsule endoscope inside gastrointestinal tract", 2014 36th Annual International Conference of the IEEE Engineering in Medicine and Biology Society (EMBC), **(2014)**.
[24] D. Zeng and Y. Geng, "Content distribution mechanism in mobile P2P network", Journal of Networks, vol. 9, no. 5, **(2014)**, pp. 1229-1236.

Authors

Liang Kangyou, He was born in Guangzhou, China, in 1974.Mr.Liang is a teacher of the School of electronics and electrical engineering, Chongqing University of arts and sciences, China. Liang received his Bachelor in 1996 in welding technology and design, and his MSC in 2014 of electrical theory and new technology from Chongqing University. Liang is leading research projects related to theory analysis, test and design of circuits and systems.